DOI: 10.1021/ma1004925

Macromolecules
ARTICLE

Polymer Dynamics in Nanochannels of Porous Silicon: A Neutron Spin Echo Study

André Kusmin,*,† Simon Gruener,‡ Anke Henschel,‡ Nicolas de Souza,§ Jürgen Allgaier,† Dieter Richter,† and Patrick Huber*,‡

†*Institut für Festkörperforschung, Forschungszentrum Jülich, 52425 Jülich, Germany,* ‡*Experimental Physics, Saarland University, 66041 Saarbrücken, Germany, and* §*Jülich Centre for Neutron Science, c/o TU München, Lichtenberg Strasse 1, 85747 Garching, Germany*

Received March 3, 2010; Revised Manuscript Received May 19, 2010

ABSTRACT: Neutron spin echo spectra of poly(ethylene oxide) (PEO) melts confined in porous silicon (the mean pore diameter: 13 nm) were recorded at $Q = 0.05$, 0.08, and 0.11 $Å^{-1}$ and successfully analyzed in terms of a two-state model, where chains adsorbed to the pore walls exhibit much slower internal dynamics than in the bulk and their centers-of-mass do not move, while free chains have bulklike internal dynamics and diffuse within an infinite cylinder in the center of the pore. The radius of this cylinder was found to be 1.4 nm for PEO 3 kg/mol (3k); this corresponds to the thickness of the adsorbed layer to be approximately equal to the Flory radius. As opposed to PEO 10k, for which details on the center of mass diffusion could not be discerned, for PEO 3k the diffusion rate along the pore was found to be smaller than that in the radial direction.

Introduction

When a molecular fluid is confined in a porous medium with a pore diameter comparable to the size of its molecules, intuitively, one expects that the diffusion rate or the diffusion mechanism will differ from that in the bulk. In the extreme case, when pores are so narrow that molecules cannot pass each other, single file diffusion takes place.[1,2] In the intermediate case, when the pore diameter is several times larger than the molecule, the situation is unclear. In a simulation study[3] it was found for the diffusion of water that the diffusion rate along the pore decreases with decreasing pore diameter while the diffusion rate in the radial direction did not change and was equal to that in the bulk state. For the smallest pore diameter studied (1.5 nm) the diffusion along the pore was ≈30% slower. To the best of our knowledge, no experimental proof of this kind of anisotropy has been found so far.

The confinement of a complex fluid can be expected to affect both the center-of-mass (CM) diffusion and the internal molecular dynamics. For example, an NMR study indicated significantly different dynamics of linear polymer chains confined in mesopores with diameters ranging from 9 to 58 nm, when compared to the bulk state.[4] Specifically, the dynamics of confined chains was found to be restricted to a snakelike motion (reptation) along the chain contour within a tube having a diameter of about 0.5 nm, a value that does not depend on the pore diameter D even for diameters of $D = 15 \times R_F$, where R_F is the Flory radius (rms end-to-end distance of a polymer chain in the bulk). Only for much larger pore sizes is a crossover from confined to bulk behavior observed. This finding, termed the "corset effect", is proposed to arise from system properties like the chain uncrossability, low compressibility, and impenetrability of the pore walls. A modified chain dynamics has also been inferred from an experiment on capillary filling dynamics of nanochannels, and thus from rheological properties of confined polymers.[5] Note, however, that in those experiments assumptions regarding both the driving capillary force and the hydrodynamic velocity boundary condition (slip length) in the nanochannels have to be made. Thus the conclusions with respect to the microscopic chain dynamics are rather indirect, given the sensitivity of capillary filling dynamics on those quantities.[6,7]

The dynamics of linear polymer chains in the bulk melt has been extensively studied.[8] For short, unentangled chains (and for the chains of any length at short times) the dynamics is well described by the Rouse model.[9] Here the chains interact solely by local friction with a heat bath representing the neighboring chains. For long chains, the entanglement of a chain within the matrix of surrounding chains leads to a change in the dynamical behavior at intermediate and long times. In the reptation model the effect of the entanglement is described by a virtual tube that localizes a given chain and limits its motion to a one-dimensional Rouse motion inside the tube (local reptation) and a slow diffusive creep motion out of the tube (reptation).[10] Neutron spin echo (NSE) experiments on bulk polymer melts confirmed the reptation model and resulted in tube diameter values of about 5 nm.[11]

While there have been neutron scattering studies on dynamics of alkanes in confinement (e.g., zeolites[12] and mesoporous silica[13]), we know of only a few such studies on the dynamics of confined polymer melts.[14,15] Here we present an NSE experiment on an unentangled and an entangled melt of polyethylene oxide (PEO) with a molecular weight of 3 kg/mol and ≈10 kg/mol, respectively, confined in porous silicon with a pore diameter of ≈13 nm (a melt becomes entangled above the critical molecular weight (M_c), which is 5.9 kg/mol for PEO[16]). As opposed to zeolites or silica glasses, in porous silicon the pores run strictly perpendicular to the wafer surface. This allowed us to selectively probe molecular motions along the pore and in the radial direction, and thus to test for a dynamical anisotropy.

Theory

Basic Model. For a polymer melt, the Flory radius is $R_F = lN^{1/2}$, where N is the number of Kuhn (i.e., freely jointed) segments in the chain and l is the Kuhn segment length.

*To whom correspondence should be addressed. E-mail: A.K., a.kusmin@fz-juelich.de; P.H., p.huber@physik.uni-saarland.de.

 Published on Web 09/16/2010

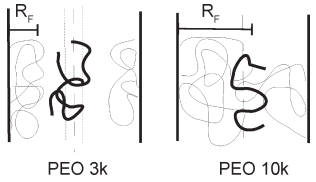

Figure 1. For PEO 3 kg/mol, free chains (thick lines) diffuse freely in the center of the pore. For PEO 10 kg/mol, free chains are entangled. PEO chains that are close to the walls are adsorbed.

Taking one segment to consist of one monomer and using $l^2 = 33.75$ Å^2,[17] R_F are 48 and 85 Å for PEO 3k and PEO 10k, respectively. The pore diameter is ≈13 nm; therefore, it is reasonable to assume that (i) confinement does not substantially perturb the chain conformation (as compared to the bulk melt); (ii) the fraction of the chains having a contact to the pore walls is not negligible. As the pore surface is covered with a silica (SiO_2) layer, and it is known that PEO adsorbs on silica through hydrogen bonds between silanol groups and ether oxygens on the polymer,[18] we expect that all PEO chains near the wall exhibit a slower dynamics than the chains in the bulk.

From the above the following basic physical model of our samples can be constructed (see Figure 1 for an illustration). For PEO 3k, there is a substantial fraction of free chains; the center of mass (CM) of these chains will diffuse as in the bulk melt, but only within a narrow cylinder in the center of the pore. On the contrary, most PEO 10k chains have some contact to the pore surface, those that are not are likely to be entangled and will diffuse primarily along the pore.

We assume that the dynamics of free chains follows the Rouse model. The dynamics of adsorbed chains is difficult to model because an adsorbed polymer layer is a mixture of trains, loops, and tails.[19,20] Since we do not know relative contributions of these three structural motifs, two further assumptions will be made: (i) the CM of an adsorbed chain does not move, and (ii) the internal dynamics of such a chain can be either neglected entirely or described by the Rouse model but with a friction coefficient that is larger than in the bulk melt. The choice of the Rouse model for both free and adsorbed chains does not influence the principal results (see Discussion).

Neutron Spin Echo. As for any other liquid, the coherent neutron scattering from a polymer melt is low at small Q values ($Q \leq 0.2$ Å^{-1}) because of the absence of a long-range order. Therefore, at small Q, the scattering by a mixture of deuterated and nondeuterated polymer chains consists almost exclusively of the single chain coherent scattering arising due to a large difference (a contrast) between the coherent scattering lengths (b) of H and D nuclei. The intensity of this scattering can be calculated by considering every hydrogen atom in a chain to have the scattering length Δb_{HD}; $(\Delta b_{HD})^2 = \langle b^2\rangle - \langle b\rangle^2 = F(1-F)(b^H - b^D)^2$, where $\langle\,\rangle$ denotes an average over all chains and F is the fraction of deuterated chains. Thus, provided the elastic scattering due to the Si matrix is negligible (see the next section), our NSE spectra represent the dynamic coherent structure factor of a polymer chain ($S(Q,t)$) normalized to its static coherent structure factor ($S(Q)$).

A general form of the $S(Q,t)/S(Q)$ expression that corresponds to the basic model described above reads

$$\frac{S(Q,t)}{S(Q)} = fS_{CM}(Q_\parallel,t)\,S_{CM}(Q_\perp,t)\frac{S_{free}(Q,t)}{S_{free}(Q)} + (1-f)\frac{S_{ads}(Q,t)}{S_{ads}(Q)} \quad (1)$$

where f is the fraction of free chains and $Q_\parallel$ and $Q_\perp$ are the Q components directed along and perpendicularly to the pore axis, respectively. We assume that the average time spent in the adsorbed state is longer than the observation time of the experiment; therefore, the exchange between the states has no effect on measured spectra. For the CM diffusion along the pore we used the model of the long-range translational diffusion[21]

$$S_{CM}(Q_\parallel,t) = \exp(-D_{TR\parallel}Q_\parallel{}^2 t) \quad (2)$$

For the CM diffusion in the direction perpendicular to the pore axis we used the model of diffusion inside a circle of a radius a[22]

$$S_{CM}(Q_\perp,t) = B_0^0(Q_\perp) + \sum_{m=1}^{\infty} B_m^0(Q_\perp)\exp[-(x_m^0)^2 D_{TR\perp}t/a^2] + 2\sum_{n=1,m=0}^{\infty,\infty} B_m^n(Q_\perp)\exp[-(x_m^n)^2 D_{TR\perp}t/a^2] \quad (3)$$

$$B_m^n(Q_\perp) = \frac{4(x_m^n)^2}{(x_m^n)^2 - n^2}\left[\frac{Q_\perp a J_{n+1}(Q_\perp a) - nJ_n(Q_\perp a)}{(Q_\perp a)^2 - (x_m^n)^2}\right]^2$$
$$B_0^0(Q_\perp) = \left[\frac{2J_1(Q_\perp a)}{Q_\perp a}\right]^2 \quad (4)$$

where J_n are the cylindrical Bessel functions of the first kind and x_m^n is the $(m+1)$th root of $(d/dx)[J_n(x)] = 0$.

The diffusion coefficients along and perpendicularly to the pore axis, $D_{TR\parallel}$ and $D_{TR\perp}$, are expected to be equal and given by the Rouse model:

$$D^{Rouse} = k_B T/N\xi_0 \quad (5)$$

where ξ_0 is the monomeric friction coefficient. The expression for the (presumably isotropic) internal chain dynamics of free chains, $S_{free}(Q,t)$, in the frame of the Rouse model reads[8]

$$S^{Rouse}(Q,t) = \sum_{i,j}\exp\left[-\frac{1}{6}Q^2|i-j|l^2 - \frac{2Q^2Nl^2}{3\pi^2}\sum_{p=1}\frac{1}{p^2}\cos\left(\frac{p\pi j}{N}\right)\cos\left(\frac{p\pi i}{N}\right)[1-\exp(-tp^2/\tau_R)]\right] \quad (6)$$

where i and j are indices for the segments. The summation over p goes over all internal Rouse modes of the polymer chain. The Rouse time, $\tau_R = \xi_0 N^2 l^2/3\pi^2 k_B T$, is the longest relaxation time of the chain with N segments. The internal dynamics of adsorbed chains was either neglected altogether (by taking $S_{ads}(Q,t)/S_{ads}(Q) = 1$) or accounted for by eq 6, with ξ_0 either being fixed to the ξ_0 value of free chains or being an independent free fitting parameter. We realize that both scenarios are unrealistic: adsorbed chains are not immobile, and their dynamics can not, in general, be modeled using eq 6. However, the structure of an adsorbed layer is complicated and our approach, although simple, was sufficient to satisfactorily describe our NSE spectra.

Problem of Elastic Scattering. At low Q, the coherent scattering from Si wafers filled with a mixture of deuterated and nondeuterated polymer chains is a sum of the elastic scattering arising due to a nonuniform distribution of the coherent scattering length density (SLD), and the (quasielastic) coherent single chain scattering due to the scattering contrast between H and D nuclei. Thus, a prerequisite for the analysis of neutron diffraction and NSE spectra in terms of the structure and dynamics of polymer chains is either a negligible

contribution of the elastic scattering or the correction for this contribution before (or in the course of) the analysis.

The coherent elastic scattering from Si wafers can be presented as (eq 45 in ref 23)

$$I(Q) = (\Delta\rho)^2 I_0(Q) + \Delta\rho I_{01}(Q) + I_1(Q) \quad (7)$$

where $\Delta\rho$ is the scattering contrast, i.e., the difference between the average SLDs of the Si matrix and the pore content. [This can be shown by writing the SLD of a wafer as $\rho(\mathbf{r}) = (\Delta\rho)\rho_c(\mathbf{r}) + \rho_1(\mathbf{r})$ and performing the Fourier transformation of $\rho(\mathbf{r})\rho^*(\mathbf{r})$. $\rho_c(\mathbf{r})$ is 1 if $\mathbf{r}$ points to a volume element inside of a pore and 0 otherwise.] If the matrix had no inhomogeneities and pores were fully filled by a homogeneous medium, the total scattering would be just $(\Delta\rho)^2 I_0(Q)$. In reality, the terms $I_{01}(Q)$ and $I_1(Q)$ are non-negligible due to a nonuniform distribution of the SLD in the matrix as well as in the pore content; the greater the size of inhomogeneities, the smaller are Q values at which $I_{01}(Q)$ and $I_1(Q)$ begin to substantially contribute to the total scattering. Inhomogeneities may have different sources (e.g., the SiO_2 layer on the surface of the pores) and may lead to a significant elastic scattering contribution even when the contrast is matched (i.e., when $\Delta\rho = 0$).

Because of inhomogeneities and a never-perfect contrast matching, one has to make sure that the residual elastic scattering is negligible in the Q region of interest. This can be done by fitting a theoretical expression for the coherent scattering by a single chain, $S^{\mathrm{Chain}}(Q)$, to the experimental coherent scattering, $I^{\mathrm{Exp}}(Q)$. If the fit quality is good and fitted values of structural parameters are correct/reasonable, any residual elastic scattering *with a Q dependence different from that of* $S^{Chain}(Q)$ is negligible. However, to exclude the possibility that there is a substantial scattering contribution due to the residual elastic scattering having a $S^{\mathrm{Chain}}(Q)$-like Q dependence, $I^{\mathrm{Exp}}(Q)$ curves have to be transformed to an absolute scale. An alternative approach, an "internal" normalization,[24] consists of the normalization of $I^{\mathrm{Exp}}(Q)$ to the spin-incoherent scattering intensity ($I_{\mathrm{inc}}^{\mathrm{Exp}}(Q)$). Specifically, one can write

$$I^{\mathrm{Exp}}(Q) = n_{\mathrm{Chain}} S^{\mathrm{Chain}}(Q) F_{\mathrm{Sc}} + B(Q) \quad (8a)$$

$$I_{\mathrm{inc}}^{\mathrm{Exp}}(Q) = n_{\mathrm{Chain}} S_{\mathrm{inc}}^{\mathrm{Chain}}(Q) F_{\mathrm{Sc}} + B_{\mathrm{inc}}(Q) \quad (8b)$$

where n_{Chain} is the chain number density, $S_{\mathrm{inc}}^{\mathrm{Chain}}$ is the theoretical spin-incoherent single chain scattering, F_{Sc} is a scaling factor converting calculated intensities into the experimental units, and $B(Q)$ and $B_{\mathrm{inc}}(Q)$ are the coherent and incoherent scattering from Si wafers, respectively, including any residual elastic scattering. From eqs 8a and 8b we get

$$I^{\mathrm{Exp}}(Q) = \frac{S^{\mathrm{Chain}}(Q)}{S_{\mathrm{inc}}^{\mathrm{Chain}}} (I_{\mathrm{inc}}^{\mathrm{Exp}}(Q) - B_{\mathrm{inc}}(Q)) + B(Q) \quad (9)$$

If $B_{\mathrm{inc}}(Q)$ and $B(Q)$ are negligible, eq 9 has no free parameters because both $I^{\mathrm{Exp}}(Q)$ and $I_{\mathrm{inc}}^{\mathrm{Exp}}(Q)$ can be obtained from a polarized neutron diffraction experiment, and $S^{\mathrm{Chain}}(Q)$ and $S_{\mathrm{inc}}^{\mathrm{Chain}}$ are given by

$$S^{\mathrm{Chain}}(Q) = N^2 n^2 (\Delta b_{\mathrm{HD}})^2 f_{\mathrm{Debye}}(Q^2 R_g^2)$$

$$\text{where} \quad f_{\mathrm{Debye}}(x) = \frac{2}{x^2}(e^{-x} - 1 + x) \quad (10a)$$

$$S_{inc}^{Chain}(Q) = Nn\langle\sigma_{inc}\rangle/4\pi \quad (10b)$$

where n is the number of H atoms per segment, $\langle\sigma_{\mathrm{inc}}\rangle$ is the incoherent cross-section of H atoms (average over all chains), and R_g is the radius of gyration (for a freely jointed chain, $R_g^2 = Nl^2/6$). A test whether $B_{\mathrm{inc}}(Q)$ is negligible can be done by fitting eq 9 to the $I^{\mathrm{Exp}}(Q)$ curves and comparing fitted ($I_{\mathrm{inc}}^{\mathrm{Exp}}(Q) - B_{\mathrm{inc}}(Q)$) values with measured ones.

Experimental Section

The polymers hPEO (protonated) and dPEO (deuterated) were prepared by anionic polymerization. Deuterated ethylene oxide was purchased from Campro Scientific (deuteration degree 99%). The triethylene glycol partially metalated with potassium was used as an initiator, as a result, dPEO chains had a non-deuterated $(-C_2H_4O-)_3$ fragment in the middle. The molar masses (M_n [g/mol]) and polydispersities (M_w/M_n) were respectively 2940 and 1.02 for hPEO 3k; 3170 and 1.02 for dPEO 3k; 9290 and 1.01 for hPEO 10k; and 9560 and 1.01 for dPEO 10k.

The porous silicon membranes are produced in-house employing an electrochemical anodic etching process of Si (100) wafer (thickness ~0.5 mm). The pores are linear, noninterconnected and oriented along the ⟨100⟩ Si crystallographic direction (perpendicular to the membrane surface) with a length of ~0.3 mm. After a special treatment with hydrofluoric acid and hydrogen peroxide the pores have a roughly circular cross-section with mean diameter ~13 nm[25] and their walls are covered with silica rendering them highly hydrophilic. The porosity of the porous layer is about 0.55.

The wafers with a polymer powder spread on the top were placed on a hot plate and left there for half an hour (PEO 3k) and > 12 h (PEO 10k). We determined the mass of the polymer taken up by the wafers; the porosity calculated from this mass indicates that the pores were (nearly) fully filled. As the filling procedure was done under the nitrogen atmosphere, we do not expect any significant degradation of the polymer.

Our PEO samples had 27% dPEO (by mass); such a composition was chosen to match the coherent scattering length density (SLD) of the polymer melt to that of the silicon matrix, and thus to suppress the elastic scattering (SLD of pure Si is 2.07 [10^{10} cm^{-2}]).

The experiment was performed at J-NSE, the NSE instrument at FRM II (Munich, Germany), at two neutron wavelengths (λ), 8 and 12.8 Å, covering the Fourier time range from 0.1 to 30 ns and from 45 to 110 ns, respectively. All measurements were done for two sample orientations per every scattering angle (θ) and, thus, per every Q value (Q is the neutron wave vector transfer, $Q = 4\pi/\lambda \sin(\theta/2)$). The experimental setup and the sample orientations are shown in Figure 2.

We recorded NSE spectra at Q = 0.05, 0.08, and 0.11 Å^{-1} for the six wafers filled with PEO 3k at 150 and 180 °C and the six wafers with PEO 10k at 100 °C. The $S(Q,t)/S(Q)$ data were corrected for resolution and the cryostat scattering using the NSE spectra of the activated-carbon powder and the cryostat recorded for the identical instrument setup. (For PEO 3k, at 180 °C and Q = 0.11 Å^{-1} the measurement was done only with λ = 8 Å.)

We also recorded diffraction intensities with π flipper turned off and on, $I\uparrow(Q)$ and $I\downarrow(Q)$, respectively, for two sets of empty Si wafers, and for the same sets after they were filled with polymer. The Q range was from 0.05 to 0.12 Å^{-1}. From $I\uparrow(Q)$ and $I\downarrow(Q)$ we calculated the coherent scattering, $I^{\mathrm{Exp}}(Q)$, and the spin-incoherent scattering, $I_{\mathrm{inc}}^{\mathrm{Exp}}(Q)$ (details on the calculation can be found elsewhere[24]). $I\uparrow(Q)$ and $I\downarrow(Q)$ for the empty cryostat were not measured, and $I^{\mathrm{Exp}}(Q)$ and $I_{\mathrm{inc}}^{\mathrm{Exp}}(Q)$ were not corrected for the scattering contributions due to the cryostat.

To account for the contribution of the spin-incoherent scattering (primarily due to H nuclei) to the NSE spectra (in our case, this contribution is less than 10% of the total polymer scattering for $Q < 0.12$ Å^{-1}), the $S(Q,t)/S(Q)$ corresponding to the internal chain dynamics was calculated as

$$\frac{S(Q,t)}{S(Q)} = \frac{n^2(\Delta b_{\mathrm{HD}})^2 S^{\mathrm{Rouse}}(Q,t) - (1/3)(n\langle\sigma_{\mathrm{inc}}\rangle/4\pi) S_{\mathrm{Inc}}^{\mathrm{Rouse}}(Q,t)}{S^{\mathrm{Chain}}(Q) - (1/3) S_{\mathrm{Inc}}^{\mathrm{Chain}}(Q)} \quad (11)$$

where $S^{\mathrm{Chain}}(Q)$ and $S_{\mathrm{Inc}}^{\mathrm{Chain}}(Q)$ are given by eqs 10a and eq 10b, respectively, and $S_{\mathrm{Inc}}^{\mathrm{Rouse}}(Q,t)$ is calculated from eq 6 but taking

only the terms for $i = j$. The factor $-1/3$ accounts for the change of the polarization of scattered neutrons in case of the spin-incoherent scattering. Note that for $t = 0$, and at large N, $S^{\mathrm{Rouse}}(Q,t)$ is equal to $S^{\mathrm{Chain}}(Q)$ given by eq 10a, except for the factor $n^2(\Delta b_{\mathrm{HD}})^2$ (this factor was omitted in eq 6 because it is canceled out by $S(Q,t)/S(Q)$ when the spin-incoherent scattering is negligible).

When eq 9 was fitted to $I^{\mathrm{Exp}}(Q)$ curves, the calculated intensity was also multiplied by the first-order transmission factor, $H_1(\alpha,\theta)$, calculated for the model of an infinite plain slab,[26] and by the factor accounting for the neutrons missing the sample in case of 45° orientation (S_{corr}).

Results

Checking Elastic Scattering Contribution. To test whether the elastic scattering contribution to our NSE spectra is negligible we fitted eq 9 to the coherent scattering from PEO 3k- and PEO 10k-filled wafers. $B(Q)$ (which contains the residual elastic scattering) was fixed at zero, and the only free fitting parameter was the experimental spin-incoherent scattering from polymer chains, that is, $I^{\mathrm{Exp}}_{\mathrm{inc}}(Q) - B_{\mathrm{inc}}(Q)$. Here $B_{\mathrm{inc}}(Q)$ is the spin-incoherent scattering contribution from the cryostat and empty Si wafers; it was not negligible compared to the spin-incoherent scattering from PEO alone. The fit range was $Q \geq 0.08$ Å^{-1}. [While the cryostat scattering accounts for about 15% of $I^{\mathrm{Exp}}(Q)$ at $Q = 0.05$ Å^{-1}, its contribution decreases to $\leq 5\%$ for $Q \geq 0.08$ Å^{-1}.]

As seen from Figure 3, at low Q the relative difference between the fitted curves and $I^{\mathrm{Exp}}(Q)$ is smaller for 45° than for 0° for both PEO 3k and PEO 10k. This could be, to some extent, due to a residual elastic scattering that is more intense at 0° orientation. Note that while we assumed that polymer scattering is isotropic, the fitted curves for 0° and 45° orientations differ from each other; the difference is nearly Q independent and given by the factor $H_1(\alpha,\theta)S_{\mathrm{corr}}$.

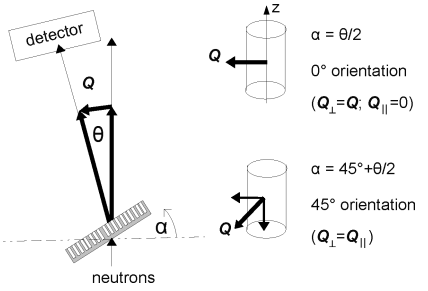

Figure 2. Left: top view of the experimental setup. For every scattering angle θ the sample (with the pores drawn as a series of white cylinders) was rotated by an angle α to adjust the orientation of the neutron wave vector transfer **Q** with respect to the pores. Right: sample orientations employed in the experiment.

A satisfactory agreement between the fitted and measured coherent scattering for $Q \geq 0.08$ Å^{-1} indicates that in this Q region a residual elastic scattering contribution with a Q dependence significantly different from that for the scattering by polymer chains is negligible. In the Supporting Information we show that a residual elastic scattering contribution can be neglected altogether.

NSE Results. All $Q = 0.05$ Å^{-1} spectra were excluded from the data analysis because of a very slow $S(Q,t)/S(Q)$ decay and significant uncertainties in the data points. As seen from the analysis of the diffraction data, this slow decay may to some extent be due to a residual elastic scattering.

As shown in Figure 2, at 0° orientation **Q** is parallel to the wafer surface. Hence, $S(Q,t)/S(Q)$ obtained for this orientation reflect the molecular motions in the plane perpendicular to the pore. At 45° orientation the molecular motions in the direction along the pore are probed as well. We assumed that the internal chain dynamics is, on average, isotropic; therefore, $Q_\perp$ and $Q_\parallel$ were only used to calculate the contribution due to the CM dynamics.

The following four models were tested: (1) no confinement, free diffusion and Rouse dynamics for all chains; (2) CM diffusion confined to an infinite cylinder (of a radius R_{D}), Rouse dynamics for all chains; (3) no confinement, free diffusion and Rouse dynamics for the free chains (f is the fraction of the free chains), the CM of an adsorbed chain being immobile; (4) CM diffusion confined to an infinite cylinder, Rouse dynamics for the free chains, the CM of an adsorbed chain being immobile. For models 3 and 4, the internal dynamics of adsorbed chains was either neglected or described by the Rouse model. In the latter case the ξ_0 value for adsorbed chains was either kept equal to that for free chains or was an independent fitting parameter.

For both PEO 3k and PEO 10k, whether we fitted the 0° orientation spectra alone, or together with the spectra for the 45° orientation, model 4 provided the best results. Other models led to a significantly worse fit quality (judging by the χ^2 value and the goodness-of-fit criterion). When we fitted model 4 to the PEO 3k spectra for both 0° and 45° orientation *simultaneously*, the fit quality improved substantially when the diffusion coefficient along the pore, $D_{\mathrm{TR}\parallel}$, was allowed to be a free parameter; its fitted value turned out to be smaller than the diffusion coefficient in the radial direction, $D_{\mathrm{TR}\perp}$ (which is given by the Rouse model, eq 5). For PEO 10k, making $D_{\mathrm{TR}\parallel}$ a free fitting parameter did not lead to a significant improvement of the fit quality; therefore, we continued to assume that $D_{\mathrm{TR}\parallel} = D_{\mathrm{TR}\perp} = D^{\mathrm{Rouse}}$.

When we fitted model 4, the best fit quality was obtained with ξ_0 for the free and adsorbed chains being two separate free fitting parameters; a slightly worse quality resulted when the internal dynamics of adsorbed chains was neglected

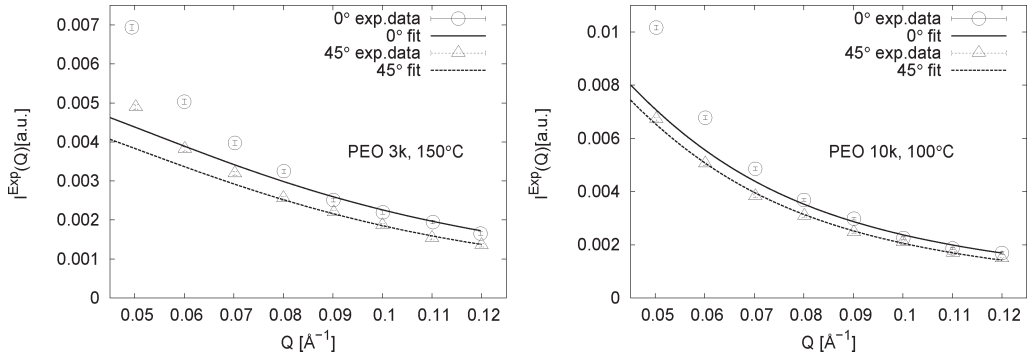

Figure 3. Results of the fit of eq 9 to the experimental coherent scattering with the residual elastic scattering contribution set to zero. The fit range was $Q \geq 0.08$ Å^{-1}.

Table 1. Results of Fitting of Model 4 to the NSE Spectra of PEO 3k and PEO 10k[a]

sample	T (°C)	orientation	R_D	ξ (10^{-20} kg/ns)	f	$D_{TR\parallel}/D_{TR\perp}$
PEO 3k	150	only 0°	14.1 ± 1.9	0.292 ± 0.05	0.59 ± 0.07	1
		0° and 45°	14.0 ± 2.1	0.270 ± 0.05	0.581 ± 0.08	0.123 ± 0.05
	180	only 0°	12.2 ± 4.2	0.34 ± 0.18	0.53 ± 0.19	1
		0° and 45°	13.0 ± 2.9	0.162 ± 0.05	0.41 ± 0.09	0.29 ± 0.10
PEO 10k	100	only 0°	2.5 ± 10	0.77 ± 0.9	0.43 ± 0.2	1
		0° and 45°	0.4 ± 8.4	0.44 ± 0.16	0.34 ± 0.07	1

[a] Adsorbed chains were assumed to be completely immobile. f is the fraction of free chains that have a monomeric friction coefficient ξ_0; the centers-of-mass of these chains diffuse inside an infinite cylinder of a radius R_D.

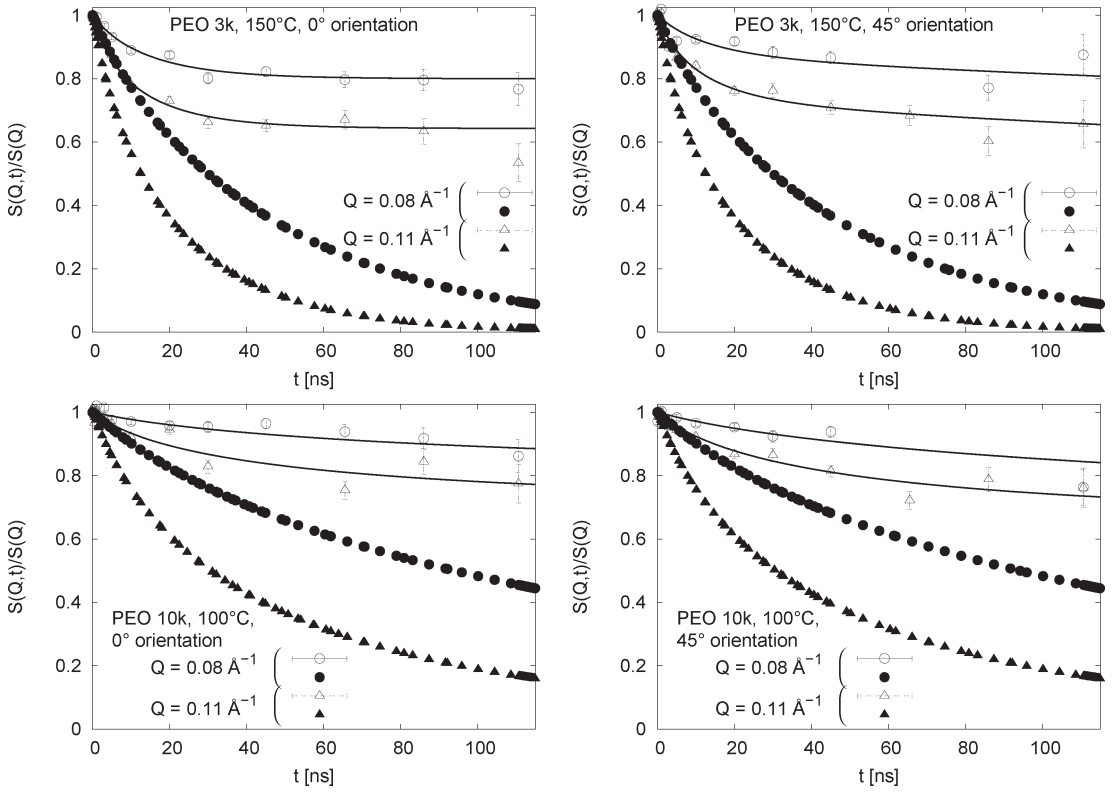

Figure 4. NSE spectra (open symbols) and the fit (lines) of model 4. The spectra for Q = 0.08 and 0.11 Å^{-1} for both 0° and 45° were fitted simultaneously; the internal dynamics of adsorbed chains was entirely neglected. ξ_0 values from these fits were used to calculate the NSE spectra for the bulk melt using model 1 (closed symbols).

altogether, and significantly worse fits were obtained when one ξ_0 was used for all, free and adsorbed, chains.

For the case when adsorbed chains were assumed to be completely immobile, the fitted values are given in Table 1, the spectra together with the fit curves are shown in Figure 4. The free fitting parameters were R_D, ξ_0, and f. For PEO 3k when both orientations were fitted simultaneously, $D_{TR\parallel}/D_{TR\perp}$ was a free parameter as well. For the case when ξ_0 for adsorbed chains was a free fitting parameter, the fit results are not shown because they are similar to the ones presented in Table 1 and Figure 4; fitted ξ_0 values for adsorbed chains were more than 10 times larger than the ξ_0 values for free chains. The fit results for the case when ξ_0 for adsorbed chains was the same as for free chains are substantially worse and therefore not shown as well.

Discussion

General Features. In the models we fitted to our NSE spectra, the internal dynamics of adsorbed chains was either neglected entirely or considered using the Rouse model for bulk polymer melts. Both approaches are oversimplifications: adsorbed chains have some internal dynamics that certainly is different from that in the bulk. However, an attempt to use a more complicated model to account for this dynamics is not justified in our case because we do not know the structure of the adsorbed polymer layer and our data set is not extensive enough to allow a definite test of such a model.

Compared to the fits of model 4 where the internal dynamics of adsorbed chains was neglected, the fits with the friction coefficient for adsorbed chains being a free fitting parameter provided similar results but only a marginally better fit quality, and while the resulting ξ_0 values were about 10 times higher than in the bulk, they had large uncertainties. Apparently, the information content of our data is not sufficient to allow one more free fitting parameter, which is coupled to the parameters that we already have. Thus, in the following, by referring to model 4, we mean model 4 together with an assumption that adsorbed chains are completely immobile.

From Figure 5 it is clear that experimental $S(Q,t)/S(Q)$ for 0° and 45° orientations are rather similar to each other. This, in principle, can be expected for short times: the molecule does not "feel" the confinement, hence, the scattering does not depend on the **Q** orientation. But for long times, assuming that the diffusion rate along and perpendicular to the pore is the same, and that the internal chain dynamics is

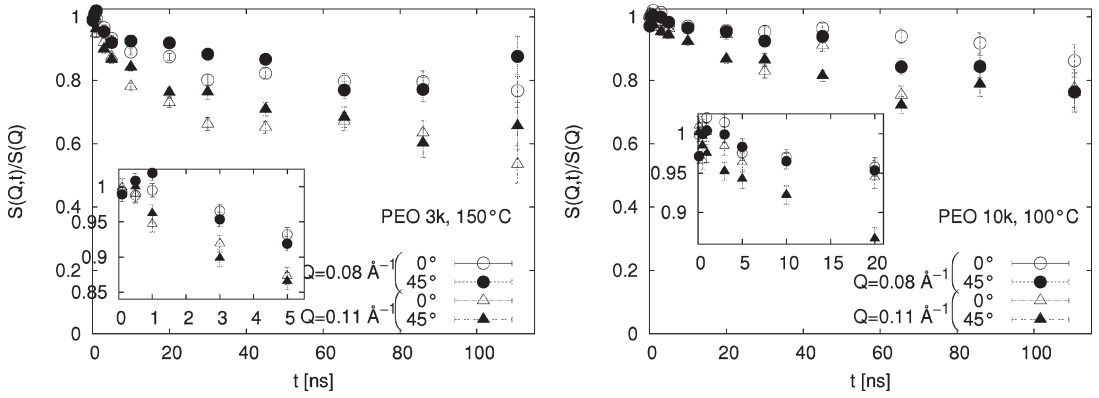

Figure 5. Comparison of NSE spectra recorded for 0° and 45° orientations. The insets contain magnified portions of respective graphs. Note that some data points shown here are not shown in Figure 4: they were influenced by magnetic disturbance and therefore excluded from fitting.

isotropic, an $S(Q,t)/S(Q)$ curve for the 45° orientation *must* monotonously decay to a lower value than is the case for the 0 orientation. The reason for this can be seen from eqs 1−4: while $S_{CM}(Q_{\parallel},t)$ decays to zero, $S_{CM}(Q_{\perp},t)$ decays to the $B_0^0(Q_{\perp})$ value, which is the elastic incoherent structure factor (EISF). Clearly, nearly identical $S(Q,t)/S(Q)$ curves for two orientations mean that either the diffusion is isotropic, but very slow, so the observation time of the experiment is not sufficient for $S_{CM}(Q_{\perp},t)$ to reach its limiting value, or the diffusion along the pore is slower than the diffusion in the radial direction. As we will see below, it appears that the first possibility is realized for PEO 10k and the second for PEO 3k.

The initial $S(Q,t)/S(Q)$ decay for the confined PEO is slower than in the bulk (see Figure 4) probably due a substantial fraction of adsorbed chains having a much slower dynamics than free chains. (At short times the dynamics free chains should not be influenced by confinement.)

The maximal thickness of an adsorbed polymer monolayer is limited by the Flory radius of a chain. Different experimental methods probe an adsorbed layer in a different way, hence, measured thicknesses vary from one method to another.[19] For example, in the case of the silica particles dispersed in aqueous solutions of PEO, the thickness of an adsorbed PEO layer was found to be $\approx R_F$ by viscometry while values systematically lower than R_F were obtained by dynamic light scattering.[27] If the pore radius (D) is known for chains such that $R_F < D/2$, the thickness of an adsorbed layer can be estimated from R_D values found by fitting model 4 to the NSE spectra; this thickness is just $D/2 - R_D$.

PEO 3k. The fitted R_D values for PEO 3k result in the thickness of the adsorbed layer equal to 51 Å ($D/2 - R_D$: 65 Å − 14 Å), a value comparable to $R_F = 48$ Å. The fitted ξ_0 values are reasonable, too: for comparison, for the bulk PEO 2.1 kg/mol at 140 °C $\xi_0 = 0.265 \times 10^{-20}$ kg/ns.[28] On the other hand, if we estimate the f value as the ratio $\pi {R_D}^2/\pi D^2$ the result is much smaller than the f values given in Table 1. However, this estimate is wrong because R_D is the radius of the cylinder where *the center-of-mass* of a free chain, and not *the whole free chain*, is confined. While in Figure 1 only small parts of free chains are outside this cylinder, it is reasonable to expect that fragments of free chains occupy a substantial fraction of the adsorbed layer. Consequently, to estimate f one must use

$$f = \frac{\pi {R_D}^2 + \pi(1-x)(D^2 - {R_D}^2)}{\pi D^2} \qquad (12)$$

where x is the volume fraction of the adsorbed layer occupied by adsorbed chains. For $D = 65$ Å, $R_D = 14$ Å, and $f = 0.59$, x is 0.43. This is a plausible value because it is known that the volume fraction $\phi(z)$ of the segments belonging to adsorbed chains is a monotonously decaying (faster than linearly) function of z.[29] Thus, the values of all fitted parameters are reasonable and compatible with the basic model constructed in the Theory section.

While model 4 provided a good description of the NSE spectra for 0° orientation, simultaneous fitting of this model to the spectra for both 0° and 45° orientations suggested a slower diffusion rate along the pore as compared to that in the radial direction; see Table 1. A similar effect was observed earlier in a molecular dynamics simulation;[30] a simple explanation is as follows. For a molecule to move along the pore, it has to push aside its neighbors in the radial direction. To move in the radial direction, it has to push aside its neighbors along the pore. Because of the walls, there is a resistance to the movement of the neighbors in the radial, but not in the axial direction. Thus, while the diffusion rate in the radial direction is essentially the same as in the bulk state, the diffusion rate in the axial direction is slower.

In principle, an exchange between the adsorbed and free states could lead to an effective diffusion rate slower than in the bulk. However, this does not appear to be the case because such an exchange (i) is probably slow and cannot be observed in the time range of our experiment and (ii) would affect the diffusion rate in both the radial and axial directions.

Assuming that diffusion along the pore and in the radial direction are not coupled (see eq 1), NSE spectra for 0° orientation are independent of the mechanism of CM diffusion along the pore. A satisfactory description of these spectra by model 4 suggests that there is no "corset effect" for PEO 3k or, at the very least, the tube diameter is ≈15 Å, and not 5 Å, as was reported for PEO 1.7 kg/mol confined in pores having a diameter of 9 nm.[4]

To check whether the above results depend on the assumption that $D_{TR\perp}$ is given by the Rouse model (i.e., eq 5), we tried to fit models 1−4 to NSE spectra of PEO 3k with $D_{TR\perp}$ being a free fitting parameter independent of the friction coefficient. In fits to the spectra for 0° orientation alone, when the fit quality was good, the resulting $D_{TR\perp}$ were similar to the value calculated from ξ_0 for the bulk PEO. In fits to the spectra for both 0° and 45° orientation, when $D_{TR\perp}$ was a ξ_0-independent free parameter, the fit quality improved significantly when we allowed for $D_{TR\parallel} \neq D_{TR\perp}$. Thus, an assumption that $D_{TR\perp}$ follows the Rouse model is reasonable, useful, but not necessary.

PEO 10k. Intuitively, model 4 is not suitable for PEO 10k. Indeed, even if there are chains that do not have a contact to the pore wall, these chains are probably entangled, and the CM diffusion does not follow the Rouse model. However,

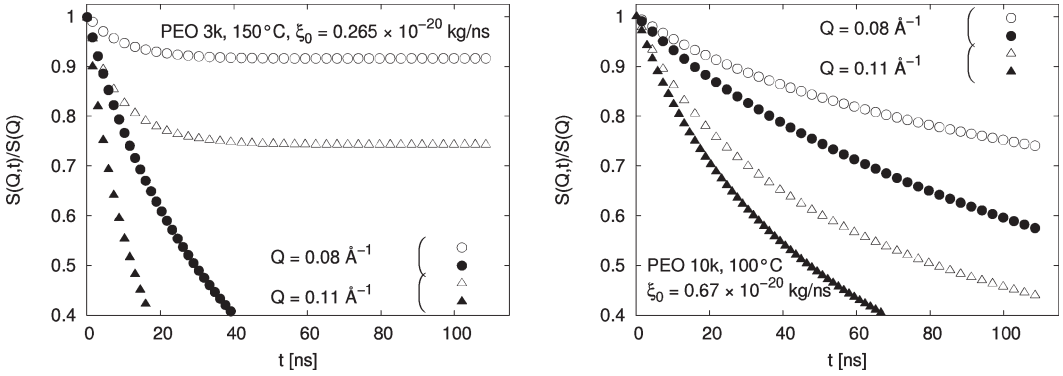

Figure 6. NSE spectra calculated for bulk PEO melts (H:D = 73:27) using model 1 (i.e., the Rouse model) with and without the contribution due to the CM diffusion (filled and open symbols, respectively). D_{TR} is given by eq 5. The spin-incoherent scattering was taken into account.

model 4 satisfactorily describes our PEO 10k spectra (Figure 4), and fitted parameter values are reasonable (for comparison, for the bulk PEO 24 kg/mol at 102 °C $\xi_0 = 0.67 \times 10^{-20}$ kg/ns[17]). For PEO 10k, $S(Q,t)/S(Q)$ spectra depend on the internal chain dynamics to a greater extent than for PEO 3k (see Figure 6). Since the actual diffusion coefficient of PEO 10k is smaller than the value predicted by the Rouse model (because of entanglements), spectra of confined PEO 10k in our time range will depend almost entirely on the internal dynamics. Thus, model 4 is not "too wrong" in our case because the details of the CM diffusion do not matter anyway, this is reflected in the weak sensitivity of the fit quality to R_D; see Table 1. Because of the slow CM diffusion, longer Fourier times (than for PEO 3k) have to be reached before a diffusional anisotropy is detectable for PEO 10k.

Internal Dynamics of Adsorbed Chains. Neglecting the internal dynamics of adsorbed chains entirely led to only slightly worse fits than in the case when a friction coefficient for adsorbed chains was a free fitting parameter. Clearly, this neglect is not a bad approximation for our samples and the Q region, at least not for PEO 3k. This can be seen from the comparison of the total $S(Q,t)/S(Q)$ decay with a decay due to the internal dynamics alone (Figure 6).

For the bulk PEO 3k, even for the long times $t \gg \tau_R$, the $S(Q,t)/S(Q)$ due to the internal dynamics alone is 0.75 at $Q = 0.11$ Å^{-1}. Given that a fraction of adsorbed chains is 0.4, and assuming that the internal dynamics of adsorbed chains is several times slower than in the bulk, its contribution to the total $S(Q,t)/S(Q)$ decay may indeed be approximated by unity (that is, no internal dynamics at all). For the bulk PEO 10k melt the relative contribution of the internal dynamics is more substantial, hence, in this case, neglecting the internal dynamics of adsorbed chains is a poorer approximation.

An adequate description of the internal dynamics of adsorbed chains is increasingly more important not only with increasing molecular weight but also with increasing Q. In a neutron scattering study on the local dynamics of PEO 43 kg/mol ($R_F \approx 18$ nm) confined in pores having a diameter ≈40 nm it was found that the confinement had little effect on the segmental dynamics for 0.2 Å^{-1} < Q < 1 Å^{-1}.[14] However, in the low Q range, as in our case, it is the large amplitude internal motions that contribute substantially; these motions may well be slowed down, and consequently, neglecting the internal dynamics of adsorbed chains is more justified.

Finally, we showed that at least for PEO 3k the spectra are rather insensitive to the details of the internal dynamics and are governed by the three major effects: geometrical confinement, PEO−surface interactions, and CM diffusion. Thus, the conclusions below are qualitatively independent of our assumption that the Rouse model can be used for both free and adsorbed chains.

Conclusion

To study the large scale polymer dynamics under confinement and to test whether this dynamics is isotropic, the NSE spectra of porous silicon wafers filled with PEO 3 kg/mol and PEO 10 kg/mol were recorded at two sample orientations. The spectra were analyzed in the frame of a two-state model where free chains undergo Rouse dynamics and diffuse within an infinite cylinder in the center of the pore and adsorbed chains have immobile center-of-mass and substantially slower (relative to free chains) internal dynamics. For both PEO 3k and PEO 10k the internal dynamics of free chains was apparently unaffected by the confinement, as evidenced by the friction coefficient similar to the values reported for the bulk PEO melts. For PEO 3k, the radius of the infinite cylinder was found to be 1.4 nm; this corresponds to the thickness of an adsorbed layer approximately equal to the Flory radius. Also for PEO 3k, the diffusion rate along the pore was found to be slower than in the radial direction. This anisotropy may be due to an effect predicted by an earlier study:[3] for a molecule to move along the pore (or in the radial direction) neighboring molecules must make space by moving in the radial direction (or along the pore); because of the walls, there is a resistance to their movement in the radial, but not in the axial, direction. For PEO 10 kg/mol the details on the CM diffusion could not be discerned.

From a more general perspective our results regarding the self-diffusion dynamics of PEO in aligned mesopores highlight a partitioning of the pore-confined polymers in two species with regard to their microscopic dynamics: A component with reduced dynamics in the pore wall proximity and a component with an unaltered dynamics in the pore center. The shear viscosity and thus the flow properties of polymers confined in such channels are intimately related to their microscopic dynamics. Therefore, our finding is of importance not only for the equilibrium physics of this system but also for the nonequilibrium transport behavior of polymers across silicon mesopores. A reduced chain dynamics in the boundary layer, and thus an increased viscosity of the molecules adjacent to the pore walls (sticky boundary layer), will lead to significantly reduced permeabilities of silicon meso- and nanopores.[6,7] For the future it would be particularly interesting to investigate how changes in the pore wall/polymer interaction, e.g., introduced by a silanization of the pore walls, affect the findings on PEO dynamics in porous silicon reported here.

Acknowledgment. A.K. thanks O. Holderer and M. Monkenbusch for the help with getting familiar with NSE in general and J-NSE in particular. This work has been supported by the German Research Foundation (DFG) within the priority program SP 1164, Nano- and Microfluidics, Grant No. Hu 850/2.

Supporting Information Available: Use of eq 9 in checking a residual elastic scattering contribution to the NSE spectra and the proof that such a contribution can be neglected. This material is available free of charge via the Internet at http://pubs.acs.org.

References and Notes

(1) Kukla, V.; Kornatowski, J.; Demuth, D.; Gimus, I.; Pfeifer, H.; Rees, L. V. C.; Schunk, S.; Unger, K. K.; Karger, J. *Science* **1996**, *272*, 702–704.
(2) Burada, P. S.; Hanggi, P.; Marchesoni, F.; Schmid, G.; Talkner, P. *ChemPhysChem*. **2009**, *10*, 45–54.
(3) Cui, S. T. *J. Chem. Phys*. **2005**, *123*, 054706.
(4) Fatkullin, N.; Fischer, E.; Mattea, C.; Beginn, U.; Kimmich, R. *ChemPhysChem*. **2004**, *5*, 884–894.
(5) Shin, K.; Obukhov, S.; Chen, J. T.; Huh, J.; Hwang, Y.; Mok, S.; Dobriyal, P.; Thiyagarajan, P.; Russell, T. P. *Nat. Mater*. **2007**, *6*, 961–965.
(6) Dimitrov, D. I.; Milchev, A.; Binder, K. *Phys. Rev. Lett*. **2007**, *99*, 054501.
(7) Gruener, S.; Huber, P. *Phys. Rev. Lett*. **2009**, *103*, 174501.
(8) Doi, M.; Edwards, S. F. *The Theory of Polymer Dynamics*; Clarendon Press: Oxford, U.K., 1986.
(9) Rouse, P. E. *J. Chem. Phys*. **1953**, *21*, 1272–1280.
(10) De Gennes, P. G. *J. Phys*. (*Paris*) **1981**, *42*, 735–740.
(11) Schleger, P.; Farago, B.; Lartigue, C.; Kollmar, A.; Richter, D. *Phys. Rev. Lett*. **1998**, *81*, 124–127.
(12) Jobic, H.; Farago, B. *J. Chem. Phys*. **2008**, *129*, 171102.
(13) Baumert, J.; Asmussen, B.; Gutt, C.; Kahn, R. *J. Chem. Phys*. **2002**, *116*, 10869–10876.
(14) Krutyeva, M.; Martin, J.; Arbe, A.; Colmenero, J.; Mijangos, C.; Schneider, G. J.; Unruh, T.; Su, Y. X.; Richter, D. *J. Chem. Phys*. **2009**, *131*, 174901.
(15) Martin, J.; Krutyeva, M.; Monkenbusch, M.; Arbe, A.; Allgaier, J.; Radulescu, A.; Falus, P.; Maiz, J.; Mijangos, C.; Colmenero, J.; Richter, D. *Phys. Rev. Lett*. **2010**, *104*, 197801.
(16) Fetters, L. J.; Lohse, D. J.; Milner, S. T.; Graessley, W. W. *Macromolecules* **1999**, *32*, 6847–6851.
(17) Niedzwiedz, K.; Wischnewski, A.; Pyckhout-Hintzen, W.; Allgaier, J.; Richter, D.; Faraone, A. *Macromolecules* **2008**, *41*, 4866–4872.
(18) Iler, R. K. *The Chemistry of Silica*; Wiley: New York, 1979.
(19) De Gennes, P. G. *Adv. Colloid Interface Sci*. **1987**, *27*, 189–209.
(20) Granick, S. *Eur. Phys. J. E*. **2002**, *9*, 421–424.
(21) Bee, M. *Quasielastic Neutron Scattering*; Bristol: Philadelphia, PA, 1988.
(22) Dianoux, A. J.; Pineri, M.; Volino, F. *Mol. Phys*. **1982**, *46*, 129–137.
(23) Stuhrmann, H. B.; Miller, A. *J. Appl. Crystallogr*. **1978**, *11*, 325–345.
(24) Zajac, W.; Gabrys, B. J.; Scharpf, O.; Andersen, K. H.; Parsonage, E. E. *Solid State Ionics* **2002**, *147*, 213–223.
(25) Kumar, P.; Hofmann, T.; Knorr, K.; Huber, P.; Scheib, P.; Lemmens, P. *J. Appl. Phys*. **2008**, *103*, 024303.
(26) Sears, V. F. *Adv. Phys*. **1975**, *24*, 1–45.
(27) Lafuma, F.; Wong, K.; Cabane, B. *J. Colloid Interface Sci*. **1991**, *143*, 9–21.
(28) Reference 17, note that $\xi_0 = 0.265 \times 10^{-20}$ kg/ns follows from the Rouse rate $W/^4 = 21\,750$ Å^4/ns mentioned in the text, while the ξ_0 value given in Table 3 (0.225) is apparently a misprint.
(29) Fleer, G. J.; Cohen Stuart, M. A.; Vincent, B.; Cosgrove, T.; Scheutjens, J. M. H. M. *Polymers at Interfaces*; Chapman and Hall: London, 1993.
(30) Reference 3, Figure 4.